

# The Jieduan-Niwan Formula Reduces Inflammatory Responses in Acute-on-Chronic Liver Failure Rats by Inhibiting HMGB1-Induced Hepatocyte Pyroptosis

Weixin Hou<sup>1,2</sup>, Peng Fang<sup>3</sup>, Jiajun Liang<sup>4</sup>, Xiaoyi Wei<sup>5</sup>, Chongyang Ma<sup>6,7</sup>, Yanbin Gao<sup>8,9</sup>, Qiuyun Zhang<sup>6,7,\*</sup>, Jingnan Li<sup>1,2,\*</sup>

<sup>1</sup>Department of Gastroenterology, Peking Union Medical College Hospital, Chinese Academy of Medical Sciences, Beijing, People's Republic of China;

<sup>2</sup>Key Laboratory of Gut Microbiota Translational Medicine Research, Chinese Academy of Medical Sciences, Beijing, People's Republic of China;

<sup>3</sup>Department of Infectious Diseases, First Affiliated Hospital of Zhejiang Chinese Medical University, Hangzhou, Zhejiang Province, People's Republic of China; <sup>4</sup>Department of Hepatology, Southern Medical University Hospital of Integrated Traditional Chinese and Western Medicine, Guangzhou, Guangdong province, People's Republic of China; <sup>5</sup>Office of Science and Technology Administration, Beijing Friendship Hospital, Capital Medical University, Beijing, People's Republic of China; <sup>6</sup>Department of Hepatology, School of Traditional Chinese Medicine, Capital Medical University, Beijing, People's Republic of China; <sup>7</sup>Department of Hepatology, Beijing Key Laboratory of Traditional Chinese Medicine Collateral Disease Theory Research, Capital Medical University, Beijing, People's Republic of China; <sup>8</sup>Department of Endocrinology, School of Traditional Chinese Medicine, Capital Medical University, Beijing, People's Republic of China; <sup>9</sup>Department of Endocrinology, Beijing Key Laboratory of Traditional Chinese Medicine Collateral Disease Theory Research, Capital Medical University, Beijing, People's Republic of China

\*These authors contributed equally to this work

Correspondence: Qiuyun Zhang, Department of Hepatology, School of Traditional Chinese Medicine, Capital Medical University, No. 10 Youanmenwai, Xitoutiao, Fengtai District, Beijing, 100069, People's Republic of China, Tel +86 10 8391 1638, Email 19970059@ccmu.edu.cn; Jingnan Li, Department of Gastroenterology, Peking Union Medical College Hospital, Chinese Academy of Medical Sciences, No. 1 Shuaifuyuan, Dongcheng District, Beijing, 100730, People's Republic of China, Tel +86 10 6915 5017, Email 13240937099@163.com

**Background:** Acute-on-chronic liver failure (ACLF) is a global intractable disease. HMGB1-induced hepatocyte pyroptosis expanding inflammatory responses contributes to the pathogenesis of ACLF. The JDNW formula (JDNWF) has a significant clinical effect on ACLF, but its hepatoprotective mechanisms remain elusive.

**Purpose:** To explore the potential molecular mechanisms of the JDNWF in ACLF by HMGB1-induced hepatocyte pyroptosis.

**Methods:** Rats were divided into normal, ACLF, Caspase-1 inhibitor, HMGB1 inhibitor, JDNW, JDNW+Caspase-1 inhibitor and JDNW+HMGB1 inhibitor groups. The ACLF rat model was established by 40% carbon tetrachloride-induced liver fibrosis, followed by intraperitoneal injection of D-galactosamine and lipopolysaccharide. The liver function, coagulation function, liver pathological damage and ultrastructural changes of hepatocytes were evaluated. Triple-immunostaining of active Caspase-1, terminal deoxynucleotidyl transferase dUTP nick end labeling (TUNEL) and albumin were performed to evaluate the percentage of pyroptotic hepatocytes. Western blot, immunofluorescence, enzyme-linked immunosorbent assay (ELISA) and quantitative real-time PCR (RT-qPCR) were used to analyze the expressions of key genes and proteins in HMGB1-induced pyroptosis pathways and the level of inflammatory factors.

**Results:** The JDNWF improved liver function, coagulation function and liver pathological damage, reduced the percentage of pyroptotic hepatocytes and inflammatory responses, and down-regulated the expressions of key genes and proteins in the HMGB1-induced pyroptosis pathways in ACLF rats. The effect of the JDNWF was better than those of HMGB1 inhibitor (glycyrrhizin) and Caspase-1 inhibitor (VX-765). Compared with glycyrrhizin or VX-765, there were no significant differences in the above indicators after the JDNWF in combination with glycyrrhizin or VX-765. These results indicated that the JDNWF inhibited hepatocyte pyroptosis and liver inflammation in ACLF rats through the HMGB1-induced pyroptosis pathways.

**Conclusion:** The JDNWF protects the livers of ACLF rats by inhibiting HMGB1-induced hepatocyte pyroptosis reducing inflammatory responses, suggesting that HMGB1-induced hepatocyte pyroptosis may be a potential therapeutic target of ACLF.

**Keywords:** traditional Chinese medicine, ACLF treatment, HMGB1, pyroptosis, inflammatory response, pharmacological effect

## Introduction

Acute-on-chronic liver failure (ACLF) is a syndrome characterized by acute severe liver decompensation on the basis of chronic liver disease, it is accompanied by a systemic inflammatory response, and may develop into multiple organ failure that leaves the patient prone to secondary infections.<sup>1</sup> ACLF develops rapidly and possesses high short-term mortality.<sup>1</sup> This intractable disease greatly affects patients' quality of life and brings a burden on the medical system. Although the research on ACLF has been conducted for decades, its clinical treatment remains limited and challenging. Currently, liver transplantation is the ultimate treatment for cirrhosis and end-stage liver disease.<sup>2</sup> However, due to lack of supply sources, postoperative rejection and other factors, it has not been widely used. There is an urgent need to find effective and practical treatments for ACLF.

Traditional Chinese medicine (TCM), which has the advantages of significant curative effects, a few side effects, and low cost, has long been used as an important alternative and complementary treatment for ACLF. The pathogenesis of ACLF is extremely complicated. From the perspective of TCM, the interaction between "toxin stasis" and "a deficiency of vital energy" is the pathogenesis characteristic of ACLF.<sup>3</sup> In view of this characteristic, Qian Ying, a well-known TCM doctor, invented the Jieduan-Niwan method (JDNWM) and formula (JDNWF) to treat ACLF. The JDNWM is considered a key method to successfully remedy liver failure, and has been included in the guidelines for clinical diagnosis and treatment of ACLF in TCM.<sup>4</sup> The JDNWF has shown remarkable clinical efficacy in the treatment of ACLF.<sup>5</sup> In addition, our previous studies have confirmed the effectiveness of JDNWF in improving the 24-h survival rate,<sup>6</sup> inhibiting hepatocyte apoptosis,<sup>3,6,7</sup> promoting hepatocyte proliferation<sup>8</sup> and improving mitochondrial damage and TCA cycle<sup>9</sup> in ACLF rats. However, due to the complex composition of TCM, the potential mechanism of the JDNWF in regulating ACLF has not been fully elucidated, and it is worthy of further exploration.

Inflammatory responses are the key factors for ACLF.<sup>10</sup> High mobility group box-1 (HMGB1) could activate immune cells to produce the tumor necrosis factor- $\alpha$  (TNF- $\alpha$ ), interleukin-1  $\beta$  (IL-1 $\beta$ ) and other pro-inflammatory factors,<sup>11</sup> and induce the systemic inflammatory response syndrome (SIRS),<sup>12,13</sup> playing a key role in the development of ACLF.<sup>14,15</sup> Pyroptosis is a programmed cell death characterized by the release of inflammatory cytokines, which trigger a strong inflammatory response.<sup>16</sup> The inflammasome-mediated hepatocyte pyroptosis lead to liver inflammation, flares of inflammation that spark on a dysfunctional immune system, contribute to potentially result in organ dysfunction/failure, as seen in ACLF.<sup>17</sup> In previous studies, we have demonstrated that HMGB1-induced hepatocyte pyroptosis expands inflammatory responses to aggravate ACLF.<sup>14</sup> The purposes of the current study were (1) to evaluate the effect of the JDNWF on liver damage and liver inflammation in ACLF rats, and (2) to investigate the potential molecular mechanisms of the JDNWF in ACLF treatment through the HMGB1-induced hepatocyte pyroptosis pathways.

## Materials and Methods

### Drug Preparation

The JDNWF is composed of 10 crude drugs (Table 1) and was purchased from Beijing TongRenTang TCM hospital. The formula was decocted as depicted in a previous study.<sup>3</sup> According to the optimal dosage of 21.7g/kg/d for each rat,<sup>3</sup> the decoction was concentrated to 4.34g/mL for subsequent animal experiments.

### Analysis of Components in JDNWF by UPLC- MS/MS

The JDNWF was extracted by freeze-drying and grinding and then used for UPLC-MS/MS analysis. The samples were separated by Agilent SB-C18 column (1.8 $\mu$ m, 2.1mm $\times$ 100mm). The pure water with 0.1% formic acid(A) and acetonitrile with 0.1% formic acid(B) were selected as the mobile phase. The elution gradient conditions were: 0min, 5%B; 0–9min, 5%–95%B; 9–10min, 95%B; 10–11min, 95%–5%B; 11–14min, 5%B. The flow velocity was set to 0.35mL/min. The column oven maintained at 40°C. The injection volume was 4 $\mu$ L. The Analyst 1.6.3 software (AB Sciex) controlled the operation of both positive and negative ion modes. The ESI source operation parameters were as follows: ion source, turbo spray; source temperature 550°C; ion spray voltage (IS) 5500V (positive ion mode)/-4500V (negative ion mode); ion source gas I (GSI), gas II (GSII), curtain gas (CUR) were set at 50, 60, and 25 psi; the collision-activated dissociation was high. The instrument was tuned and calibrated with 10 and 100 $\mu$ mol/L polypropylene glycol solutions in triple quadrupole (QQQ) and LIT modes. QQQ scans were acquired as MRM experiments with collision gas (nitrogen) set to medium. Through further DP and CE optimization, DP and CE for

**Table 1** Contents of the JDNWF

Chinese Name	Latin Name	Common Name	Weight (g)	Part Used
Ku Wei Ye Xia Zhu	<i>Phyllanthus amarus</i> Schumach. and Thonn.	Carry Me Seed	30	Herb
Huang Qi	<i>Astragalus membranaceus</i> (Fisch.) Bunge	Astragalus Root	30	Root
Gua Lou	<i>Trichosanthes kirilowii</i> Maxim	Chinese Cucumber	30	Fruit
Jin Qian Cao	<i>Lysimachia christinae</i> Hance	Lysimachia	30	Herb
Hu Ji Sheng	<i>Viscum coloratum</i> (Kom.) Nakai	Chinese Mistletoe	30	Stem, leaf
Dan Shen	<i>Salvia miltiorrhiza</i> Bunge	Red Sage	20	Root
Di Huang	<i>Rehmannia glutinosa</i> (Gaertn.) DC	Dried Rehmannia Root	20	Root
Fu Zi	<i>Aconitum carmichaeli</i> Debx.	Monkshood	15	Root
San Qi	<i>Panax notoginseng</i> (Burkill) F. H. Chen	Notoginseng	6	Root
E Zhu	<i>Curcuma phaeocaulis</i> Valetan	Rhizoma Curcumae	6	Rhizome

**Abbreviation:** JDNWF, Jieduan-Niwan formula.

individual MRM transitions were completed. A specific set of MRM transitions were monitored at each period based on the metabolites eluted within this period. The identified compounds include catalpol, rehmannioside D, salvianolic acid I, notoginsenoside R1, ginsenoside Rg1, luteolin, spermine, 4-guanidinobutanol, gallic acid, 1-methoxy-indole-3-acetamide, quercetin-3-o-rutinoside, glycitin, calycosin-7-o-glucoside, kaempferol-3-o-rutinoside, formononetin-7-o-glucoside, quercetin, kaempferol, astragaloside A, tanshinone I, cryptotanshinone. Chemical mass spectra and main components information of JDNWF were shown in [Figure S1](#) and [Table S1](#).

## Animal Materials

Specific-pathogen-free (SPF) male Wistar rats (weighing 180–200g) were purchased from Beijing Vital River Laboratory Animal Technology Co., Ltd., Beijing, China. The rats were raised under SPF conditions in the Laboratory Animal Center of Capital Medical University, Beijing, China at a room temperature of 22–25°C and humidity of (50.0±2.0) %. The rats were placed in individually ventilated cages (IVC) with food and water ad libitum, and the room lighted up every 12h.

## Animal Experiments

The rats (n=73) were acclimated for 1 week and were then randomly divided into the normal group (n=8) and the treatment groups (n=65). The latter included the ACLF group (n=15), the Caspase-1 inhibitor group (n=10), the HMGB1 inhibitor group (n=10), the JDNW group (n=10), the JDNW+Caspase-1 inhibitor group (n=10) and the JDNW+HMGB1 inhibitor group (n=10). All rats in the treatment groups were established as an ACLF model according to the previously reported method ([Figure 1](#)).<sup>14,18</sup> Specifically, the treatment groups were intraperitoneally received 40% carbon tetrachloride (CCl<sub>4</sub>) and vegetable oil mixture (1.5mL/kg) twice a week, for 10 consecutive weeks. Liver biopsy was subsequently performed. Masson's trichrome (MT) and hematoxylin and eosin (HE) staining results showed that liver fibrosis occurred in the treatment groups ([Figure S2](#)). On the basis of the liver fibrosis model, the rats were intraperitoneally injected with D-galactosamine (D-GalN, 500mg/kg) and lipopolysaccharide (LPS, 100µg/kg) for acute attacks to establish the ACLF model. After acute attacks for 24 h, the JDNW group was given the JDNWF (5mL/kg) via oral gavage,<sup>3</sup> the HMGB1 inhibitor group was intraperitoneally injected with glycyrrhizin (GLY, MedChemExpress, 50mg/kg),<sup>14</sup> the Caspase-1 inhibitor group was intragastrically injected with VX-765 (MedChemExpress, 50mg/kg),<sup>14</sup> the JDNW+HMGB1 inhibitor group was intraperitoneally injected with GLY (MedChemExpress, 50mg/kg)<sup>14</sup> and then given the JDNWF (5mL/kg) via oral gavage,<sup>3</sup> the JDNW+Caspase-1 inhibitor group was intragastrically injected with VX-765 (MedChemExpress, 50mg/kg)<sup>14</sup> and the JDNWF (5mL/kg).<sup>3</sup> The above-mentioned administration was once a day for 10 consecutive days. After these 10 days, eight rats survived in the ACLF group, and seven rats survived in each of the other treatment groups. The surviving rats were sacrificed after 10 days of treatment, and blood and liver tissue samples were collected for examination.

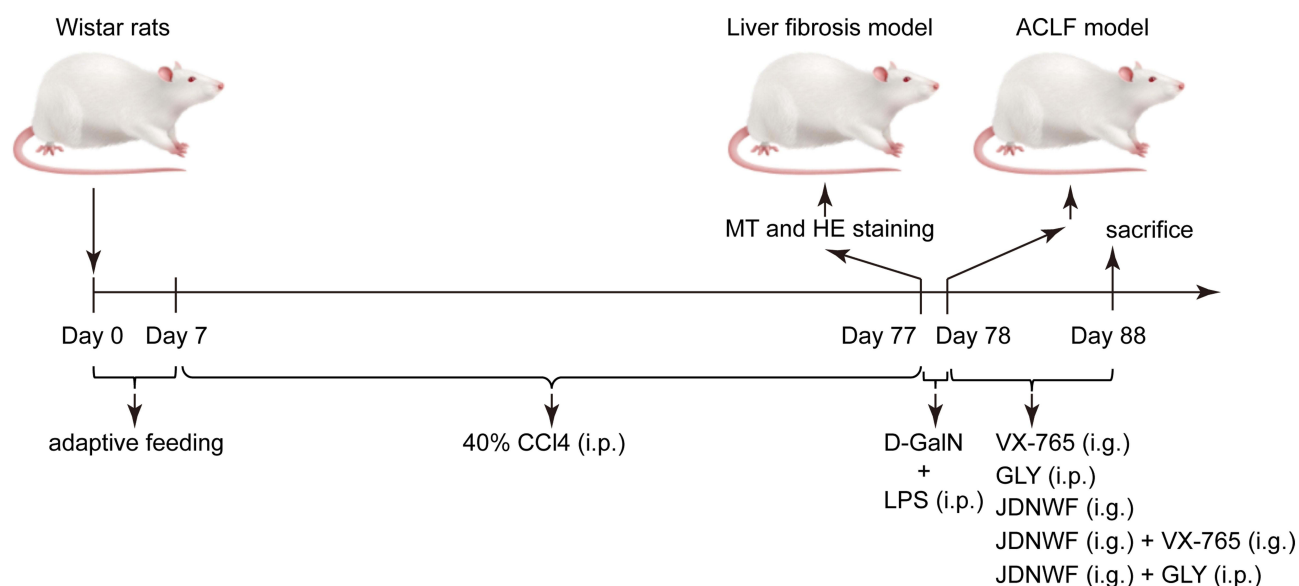


**Figure 1** Experimental flow chart of ACLF model establishment and drug administration treatment.

**Abbreviations:** ACLF, acute-on-chronic liver failure; MT staining, masson's trichrome staining; HE staining, hematoxylin and eosin staining; CCl<sub>4</sub>, carbon tetrachloride; D-GalN, D-galactosamine; LPS, Lipopolysaccharide; GLY, glycyrrhizin; JDNWF, Jieduan-Niwan formula; i.p., intraperitoneal injection; i.g., intragastric administration.

## Liver Function Test

The blood samples were centrifuged at 4000rpm for 15min at 4°C to collect the serum. Liver function was evaluated by measuring the alanine aminotransferase (ALT), aspartate aminotransferase (AST), total bilirubin (TBIL) and albumin (ALB) using a Hitachi 7600 automatic biochemical analyzer (Hitachi, Tokyo, Japan).

## Coagulation Function Test

The blood samples were centrifuged at 4000rpm for 15min at 4°C to separate the plasma. The international normalized ratio (INR) and prothrombin time (PT) were assayed by the Beckman Coulter ACL-TOP 700 Coagulation Analyzer (Beckman Coulter, Inc., Chaska, MN, USA) within 2h.

## Lactate Dehydrogenase (LDH) Release Assay

The serum LDH was evaluated using the LDH Release Assay Kit (Leadman Group Co., Ltd., Beijing, China) according to the manufacturer's instructions.

## Hepatic Pathology

The paraffin-embedded liver tissues were performed HE, MT and reticular fiber staining. Panoramic scans were performed using the Pannoramic SCAN II slide scanner (3DHISTECH Ltd., Budapest, Hungary). CaseViewer software was used to magnify the tissues 50, 100, 200, and 400 times to evaluate liver pathological changes.

## Transmission Electron Microscopy (TEM)

The livers sections stained with saturated uranyl acetate and lead citrate, and then observed under a Hitachi HT7700 TEM (Hitachi, Tokyo, Japan).

## Enzyme-Linked Immunoassay (ELISA)

The serum HMGB1, TLR4 and RAGE and the interleukin-18(IL-18), IL-1 $\beta$ , TNF- $\alpha$  and interleukin-6(IL-6) in the liver were evaluated by ELISA kits (ThermoFisher scientific, Waltham, USA). The operations were carried out in accordance with the manufacturers' instructions.



## Immunofluorescent Staining

The paraffin sections were dewaxed with xylene and gradient ethanol, and subjected to antigen retrieval by citrate buffer solution. The slices were then sealed with 10% normal goat serum at 37°C and incubated overnight in anti-HMGB1 antibody (1:250, ab79823, Abcam, Cambridge, UK) or anti-Gasdermin D (GSDMD) antibody (1:200, ab219800, Abcam, Cambridge, UK) at 4°C. The slices were incubated with Rhodamine (TRITC)-conjugated Goat Anti-Rabbit IgG(H+L) (1:50, SA00007-2, Proteintech, Chicago, IL, USA) or Fluorescein (FITC)-conjugated Affinipure Goat Anti-Rabbit IgG(H+L) (1:50, SA00003-2, Proteintech, Chicago, IL, USA) at 37°C. The slices were stained with 4',6-diamidino-2-phenylindole (DAPI), and subjected to examinations using a Leica TCS SP8 STED 3X Super-Resolution Confocal Microscope (Leica Microsystems, Wetzlar, Germany).

In addition, we performed triple-immunostaining of active Caspase-1, terminal deoxynucleotidyl transferase dUTP nick end labeling (TUNEL) and ALB (hepatocyte marker)<sup>19</sup> on slices to observe hepatocyte pyroptosis. Five slices were randomly examined from each group, and ten fields were randomly selected for each slice. The percentage of pyroptotic hepatocytes was calculated and the mean value was taken for statistical analysis.

## Western Blot Analysis

Western blot was performed as described previously.<sup>3,14</sup> In short, the total proteins were extracted from livers, and the nuclear and cytoplasmic proteins were separated with the nuclear and cytoplasmic protein extraction kits (Beyotime Biotechnology, Shanghai, China). The proteins were isolated by SDS polyacrylamide gel electrophoresis (SDS-PAGE) and transferred to polyvinylidene difluoride (PVDF) membranes. The membranes were sealed with 5% skimmed milk powder and then incubated overnight in the primary antibody diluent at 4°C. The membranes were incubated at room temperature with the secondary antibody diluent. The primary and secondary antibodies are shown in [Table S2](#). The blots were imaged by the ECL chemiluminescence (New Cell & Molecular Biotech Co., Ltd., Suzhou, China) and the Vilber FUSION FX6 XT gel chemiluminescence imaging analysis system (Vilber Lourmat, Marne La Vallée, France). The anti-Histone H3 and anti-GAPDH antibody were used as internal controls. The blot intensities were quantified with ImageJ software.<sup>20</sup> All experiments were repeated three times.

## Quantitative Real-Time PCR (RT-qPCR) Analysis

Guided by the manufacturer's instructions, the total RNAs were isolated using the RNAprep pure Tissue Kit (TIANGEN biotech Co., Ltd., Beijing, China). Then the total RNAs were reverse-transcribed into cDNA according to the instructions of the FastKing RT Kit (With gDNase) (TIANGEN biotech Co., Ltd., Beijing, China), and the SuperReal PreMix Plus (SYBR Green) Kit (TIANGEN biotech Co., Ltd., Beijing, China) was used to perform the RT-qPCR assay, with  $\beta$ -actin as internal reference. The reaction conditions were as described in a previous study.<sup>14</sup>  $2^{-\Delta\Delta CT}$  was used to analyze gene expression. All experiments were repeated three times. The primer sequences used in the experiment are shown in [Table 2](#).

## Statistical Analyses

All statistical analyses were performed using GraphPad Prism 9 (GraphPad Software, Inc., La Jolla, CA, USA). The normality of data was evaluated using the Shapiro–Wilk test and QQ plot ([Figure S3](#)). For comparison between the two groups, Student's *t*-test was used when the data followed normal distribution and showed homogeneity of variance; while the Mann–Whitney test was used when the data were not normally distributed or showed inhomogeneity of variance. For comparison among multiple groups, when the data followed normal distribution and exhibited homogeneity of variance, one-way ANOVA was performed, followed by the Tukey's test; whereas when the data were not normally distributed or showed inhomogeneity of variance, the Kruskal–Wallis test was used, followed by Dunn's test.  $P < 0.05$ ,  $P < 0.01$ ,  $P < 0.001$ , and  $P < 0.0001$  were considered as statistically significant.

## Results

### JDNWF Reduced Liver Damage of ACLF Rats

To determine the effect of the JDNWF on liver damage in ACLF rats, we evaluated the liver function, coagulation function and pathological changes. Compared with the ACLF group, the JDNWF, VX-765 and GLY significantly reduced ALT, AST, TBIL,

**Table 2** Primer Sequences for RT-qPCR Analyses

Gene Name		Primer Sequences (5' to 3')
HMGB1	Forward	5'- CGAATGTGTCTTTAGCTAGCCCTGT-3'
	Reverse	5'- CAGACTGTACCAGGCAAGGTTAGTG-3'
Caspase-1	Forward	5'- ACTCGTACACGTCTTGCCCTCA-3'
	Reverse	5'- CTGGGCAGGCAGCAAATTC-3'
NLRP3	Forward	5'- CTGAAGCATCTGCTCTGCAACC-3'
	Reverse	5'- AACCAATGCGAGATCCTGACAAC-3'
IL-1 $\beta$	Forward	5'- CCCTGAACCTCAACTGTGAAATAGCA-3'
	Reverse	5'- CCCAAGTCAAGGGCTTGAA-3'
IL-18	Forward	5'- ACTGGCTGTGACCCTATCTGTGA-3'
	Reverse	5'- TTGTGTCCTGGCACACGTTTC-3'
$\beta$ -actin	Forward	5'- CCTAAGGCCAACCCTGAAA-3'
	Reverse	5'- CAGAGGCATACAGGGACAACAC-3'

**Abbreviations:** RT-qPCR, quantitative real-time RT-PCR; HMGB1, High mobility group box-1; IL-1 $\beta$ , interleukin-1  $\beta$ ; IL-18, interleukin-18.

PT and INR, and JDNWF showed the most significant improvement (Figure 2A–C, E and F). After treatments with VX-765, GLY and the JDNWF, the ALB level was higher, but there was no statistical difference (Figure 2D). After treatments with VX-765, GLY and the JDNWF, the typical pathological damage of ACLF was alleviated, and the degree of inflammatory cell infiltration and tissue necrosis reduced, the nuclei were deformed and condensed infrequently, the mitochondrial membranes remained ruptured, but the cristae were clear, the endoplasmic reticulum (ER) dilation reduced, and the lysosomal membranes were intact, as confirmed via HE, MT, reticular fiber staining and TEM (Figure 2G–J). These results suggested that the JDNWF significantly alleviated liver damage in ACLF rats, and the effect of JDNWF is better than those of VX-765 and GLY.

## JDNWF Reduced Hepatic Inflammation in ACLF Rats

To explore the anti-inflammatory effect of the JDNWF on ACLF, we determined the expressions of inflammatory factors in the liver by the Western blot (Figure 3A–D), the RT-qPCR (Figure 3E and F) and the ELISA (Figure 3G–J). The results showed that the expressions of pro-IL-1 $\beta$ , IL-1 $\beta$ , IL-18, TNF- $\alpha$  and IL-6 were significantly higher in ACLF rats, and the expressions were notably inhibited by VX-765, GLY and JDNWF treatments, with inhibition by the JDNWF most significant. These results showed that the JDNWF alleviated hepatic inflammation in ACLF rats.

## JDNWF Decreased HMGB1 and Its Receptors TLR4 and RAGE in the Liver and Serum of ACLF Rats

Considering that HMGB1 plays a crucial role in ACLF and participates in its development,<sup>14</sup> we investigated the expression of HMGB1. The Western blot results showed that the expression of HMGB1 in the nucleus of the ACLF group decreased, while the expression in the cytoplasm increased, and HMGB1 showed obvious translocation. Importantly, the translocation of HMGB1 was suppressed by JDNWF and GLY treatments, with the suppression more obvious in the JDNW group (Figure 4A–C). The results of immunofluorescence further confirmed this phenomenon (Figure 4D). The transcript levels of *HMGB1* (Figure 4E) and the serum HMGB1 level (Figure 4F) were notably inhibited by VX-765, GLY and JDNWF treatments, with the inhibition by the JDNWF most significant, as confirmed via the RT-qPCR and ELISA. In addition, we evaluated the levels of TLR4 and RAGE—two receptors of HMGB1—in the liver and serum of ACLF rats by the Western blot and the ELISA, and the results showed that the levels of TLR4 and RAGE were reduced by VX-765, GLY and JDNWF treatments, with the decrease more obvious in the JDNW group (Figure 4G–K). These results indicated that HMGB1 was activated in ACLF rats, and the JDNWF could significantly inhibit the expression of HMGB1, TLR4 and RAGE in ACLF rats.

## JDNWF Inhibited Hepatocyte Pyroptosis in ACLF Rats

Considering that the activation of HMGB1 is closely related to hepatocyte pyroptosis,<sup>14</sup> we further explored the effect of the JDNWF on hepatocyte pyroptosis in ACLF rats. The results of the Western blot and immunofluorescence

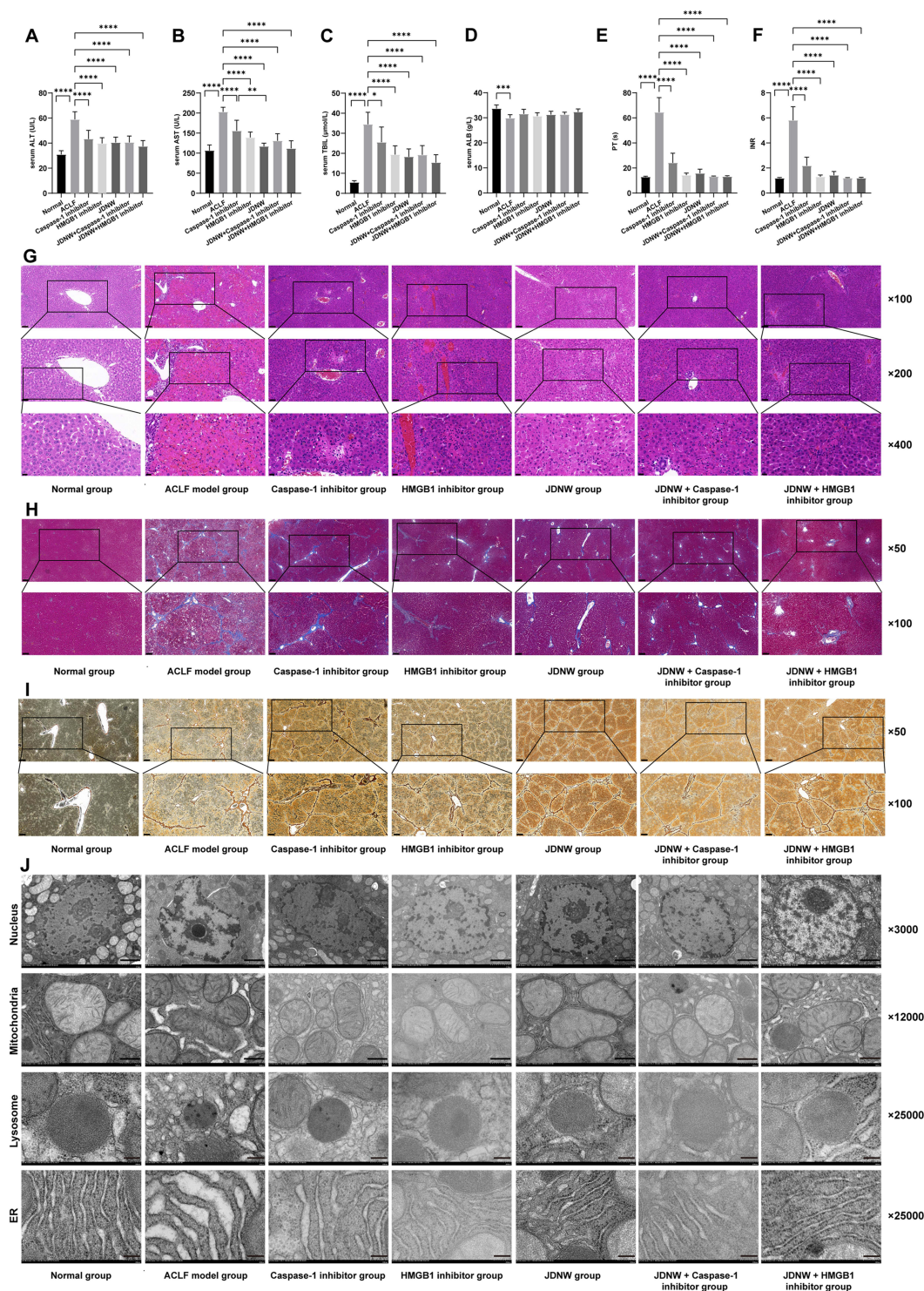


**Figure 2** JDNWF reduced liver damage of ACLF rats.

**Notes:** (A) Serum ALT level; (B) Serum AST level; (C) Serum TBIL level; (D) Serum ALB level; (E) PT in each group; (F) INR in each group.  $n=7$  per group. Asterisks indicate statistical significance:  $P<0.05$ ,  $P<0.01$ ,  $P<0.001$ , and  $P<0.0001$ . (G) HE staining of hepatic tissues (magnification,  $\times 100$ ,  $\times 200$ , and  $\times 400$ ; scale bar=100, 50, and  $20\mu\text{m}$ ). (H) MT staining of hepatic tissues (magnification,  $\times 50$  and  $\times 100$ ; scale bar=200 and  $100\mu\text{m}$ ). (I) Reticular fiber staining of hepatic tissues (magnification,  $\times 50$  and  $\times 100$ ; scale bar=200 and  $100\mu\text{m}$ ). (J) TEM was used to observe the hepatocyte nucleus, mitochondria, lysosome, and ER (magnification,  $\times 3000$ ,  $\times 12000$ ,  $\times 25000$ , and  $\times 25000$ ; scale bar= $2\mu\text{m}$ ,  $500\text{nm}$ ,  $200\text{nm}$ , and  $200\text{nm}$ ).

**Abbreviations:** JDNWF, Jieduan-Niwan formula; ACLF, acute-on-chronic liver failure; ALT, alanine aminotransferase; AST, aspartate aminotransferase; TBIL, total bilirubin; ALB, albumin; PT, prothrombin time; INR, international normalized ratio; HE staining, hematoxylin and eosin staining; MT staining, masson's trichrome staining; TEM, transmission electron microscopy; ER, endoplasmic reticulum.



showed that the expressions of GSDMD and GSDMD-N and the percentage of GSDMD positive cells were significantly higher in ACLF rats. Importantly, these effects were notably inhibited by VX-765, GLY and JDNWF treatments (Figure 5A–E). And the serum LDH level decreased by VX-765, GLY and JDNWF treatments (Figure 5F). Together with the results of pro-IL-1 $\beta$ , IL-1 $\beta$  and IL-18 (Figure 3A–H), the data suggested that the JDNWF inhibited pyroptosis in ACLF rats.

To further observe the effect of JDNWF on hepatocyte pyroptosis in ACLF rats, triple-immunostaining of active Caspase-1, TUNEL and ALB were performed, triple-positive cells are considered as pyroptotic hepatocytes. The results showed that the percentage of pyroptotic hepatocytes in ACLF rats increased significantly. Interestingly, after treatments with GLY, VX-765 and the JDNWF, the percentage decreased (Figure 5G and H). These results indicated that the JDNWF could significantly inhibit hepatocyte pyroptosis.

## JDNWF Reduced Pyroptosis in ACLF Rats by Inhibiting HMGB1-Induced Pyroptosis Pathways

To further investigate the potential molecular mechanism of the JDNWF in the regulation of pyroptosis, we evaluated the expressions of key genes and proteins in HMGB1-induced pyroptosis pathways. The results of the Western blot and the RT-qPCR showed that the expressions of NF- $\kappa$ B, NLRP3, ASC and Caspase-1 and the ratio of cleaved Caspase-1/(Caspase-1+cleaved Caspase-1) was significantly decreased by VX-765, GLY and JDNWF treatments in the liver of ACLF rats, with the decrease more obvious in the JDNW group (Figure 6A–G). Combined with the results of pro-IL-1 $\beta$ , IL-1 $\beta$ , IL-18, TNF- $\alpha$ , IL-6, GSDMD and GSDMD-N in the pathways (Figures 3A–J and 5A–E), we found that the JDNWF could reduce pyroptosis in the liver of ACLF rats by inhibiting HMGB1-induced pyroptosis pathways.

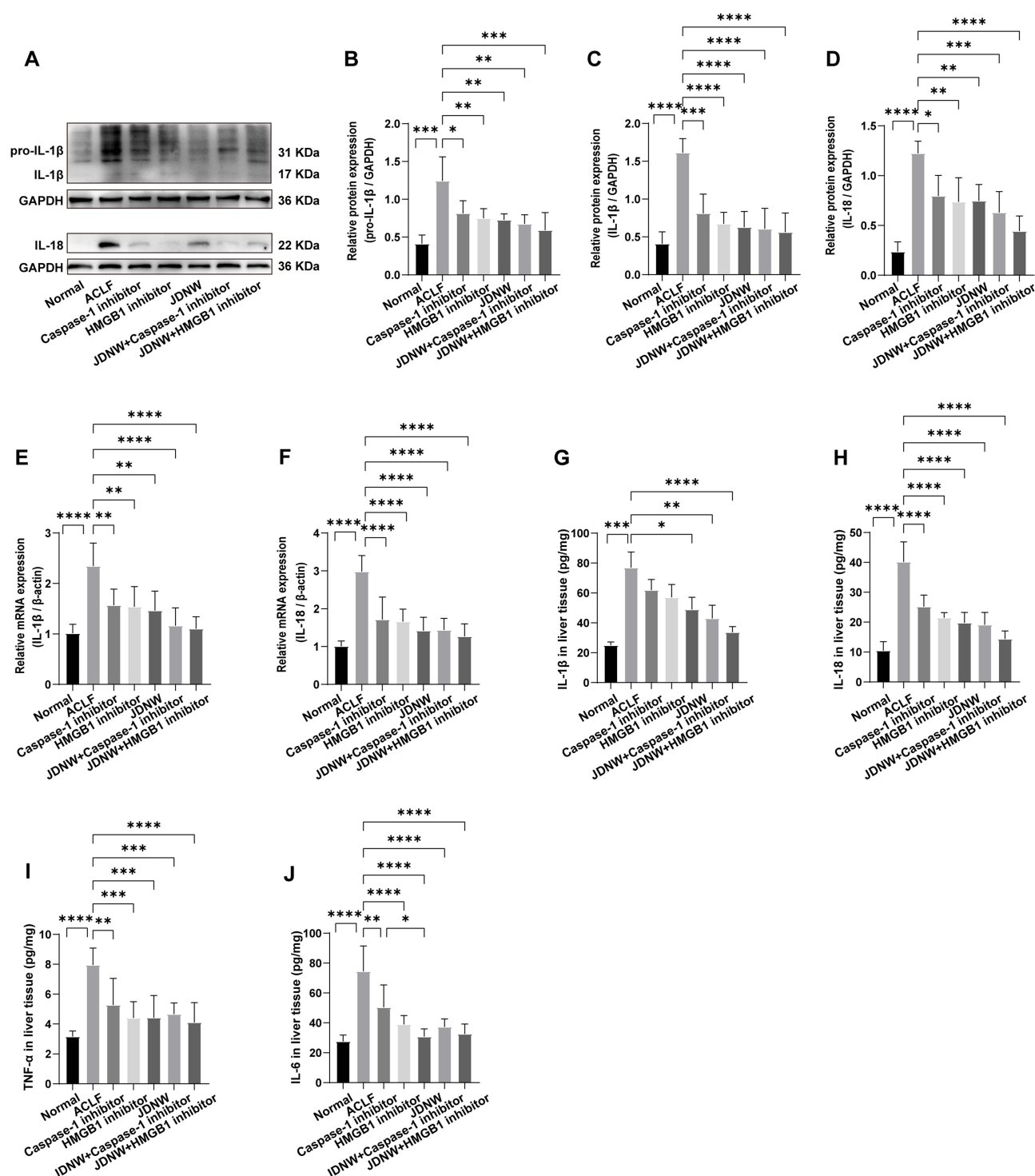
## JDNWF Exerted Hepatoprotective Effects Through HMGB1-Induced Pyroptosis Pathways in ACLF Rats

To further confirm that the JDNWF could protect the livers of ACLF rats by inhibiting the HMGB1-induced pyroptosis pathways, we established the JDNW+Caspase-1 inhibitor group and the JDNW+HMGB1 inhibitor group. The results showed that the JDNWF combined with GLY or VX-765 significantly improved liver function, coagulation function, pathological damage and ultrastructural changes in ACLF rats, and reduced inflammation, inhibited the expressions of HMGB1, TLR4, RAGE and the expressions of key genes and proteins in HMGB1-induced pyroptosis pathways. However, compared with GLY or VX-765, there were no significant differences in the above indicators after the JDNWF in combination with GLY or VX-765 (Figures 2 and 6). These results suggested that the JDNWF played a hepatoprotective role via the inhibition of the HMGB1-induced pyroptosis pathways.

## Discussion

ACLF is a major global healthcare issue. ACLF patients often show evidence of pro-inflammatory states, including local liver inflammation and SIRS.<sup>1</sup> When excessive inflammatory responses occur, cytokine storms may cause tissue damage and further development of multiple organ failure. Therefore, reducing inflammation and liver damage are essential for ACLF treatment. The JDNWF plays an important role in the clinical treatment of ACLF. It can improve the liver function of ACLF patients, relieve clinical symptoms and reduce mortality.<sup>5</sup> Our study also confirmed that the JDNWF could protect the liver function and coagulation function of ACLF rats, alleviate inflammatory cell infiltration, hepatocyte ultrastructure damage and tissue necrosis, significantly reduce the liver inflammatory factors. The improvement effects of the JDNWF were better than those of GLY or VX-765. These results indicated that the JDNWF could significantly reduce liver damage and inflammation in ACLF rats. Compared with GLY or VX-765, there were no significant differences in the above indicators after the JDNWF in combination with GLY or VX-765. These results indicated that the hepatoprotective mechanism of the JDNWF is related to HMGB1-induced pyroptosis.

In ACLF, pathogen-related molecular patterns (PAMPs) and damage-associated molecular patterns (DAMPs) activate immune cells, initiating inflammatory signals through the release of cytokines and chemokines, thereby amplifying and maintaining inflammation.<sup>1</sup> Perhaps one of the most characteristic DAMPs, HMGB1, is a highly conserved chromatin-binding protein that is usually located in the nucleus and can be secreted and released by activated immune cells and necrotic cells when





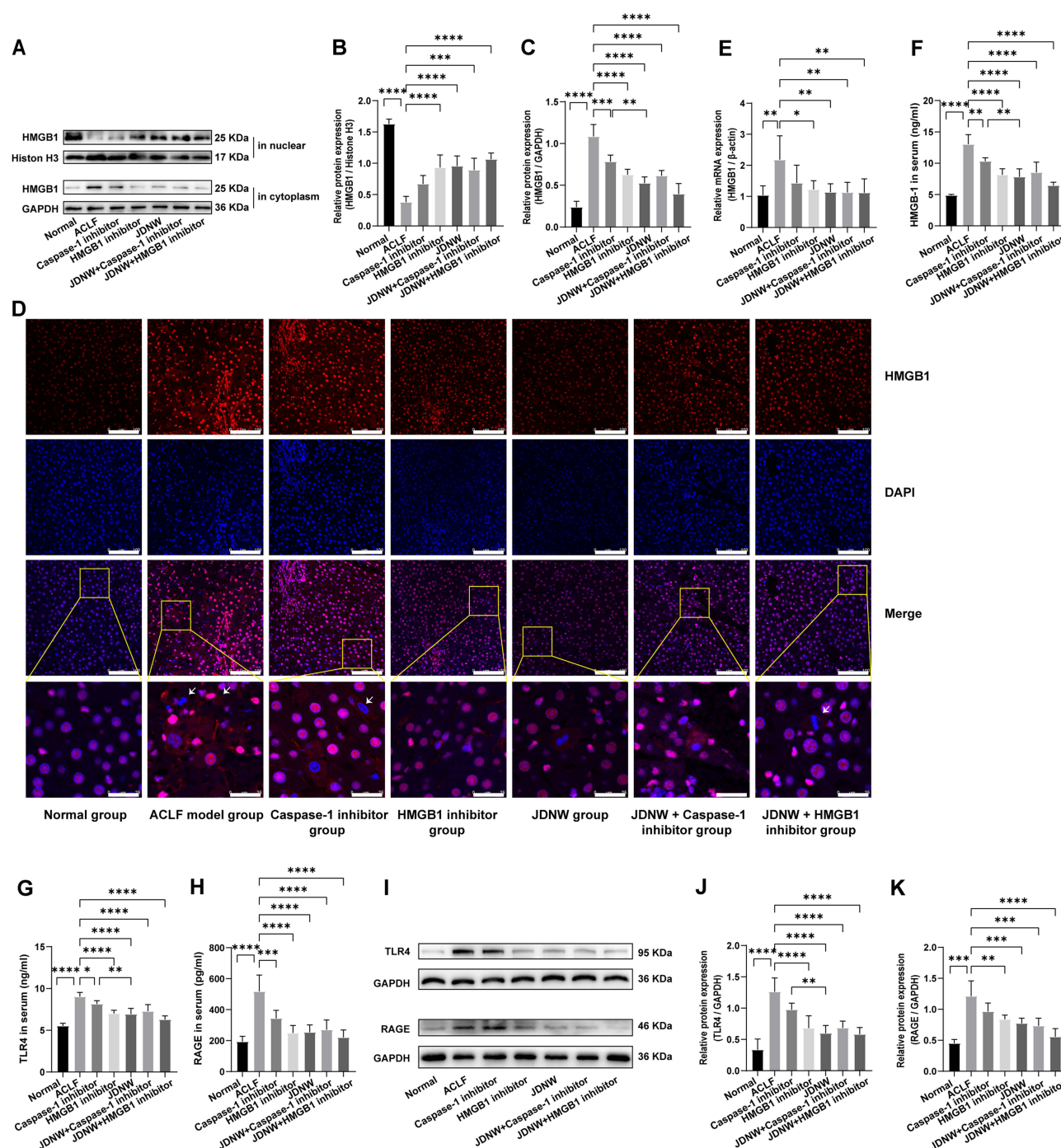


**Figure 4** JDNWF decreased HMGB1 and its receptors TLR4 and RAGE in the liver and serum of ACLF rats.

**Notes:** (A–C) The expression levels of HMGB1 in the nucleus and cytoplasm were evaluated by the Western blot. Histone H3 or GAPDH were used as the loading control. n=5 per group. (D) The expression and translocation of HMGB1 in the liver were determined by immunofluorescence (magnification,  $\times 400$ ; scale bar=100 $\mu$ m). A region is selected randomly and further enlarged below (magnification,  $\times 1600$ ; scale bar=25 $\mu$ m). The arrows represent cells that exhibited HMGB1 translocation. (E) The relative transcript level of HMGB1 of rats was detected by the RT-qPCR.  $\beta$ -actin was used as internal reference. n=6 per group. (F–H) The ELISA was used to determine the levels of HMGB1, TLR4 and RAGE in serum. n=7 per group. (I–K) The Western blot was used to detect the expressions of TLR4 and RAGE. GAPDH was used as the loading control. n=5 per group. Asterisks indicate statistical significance:  $P < 0.05$ ,  $P < 0.01$ ,  $P < 0.001$ , and  $P < 0.0001$ .

**Abbreviations:** JDNWF, Jieduan-Niwan formula; HMGB1, High mobility group box-1; TLR4, Toll-like receptor 4; RAGE, receptor for advanced glycation end-products; ACLF, acute-on-chronic liver failure; RT-qPCR, quantitative real-time RT-PCR; ELISA, enzyme-linked immunosorbent assay.

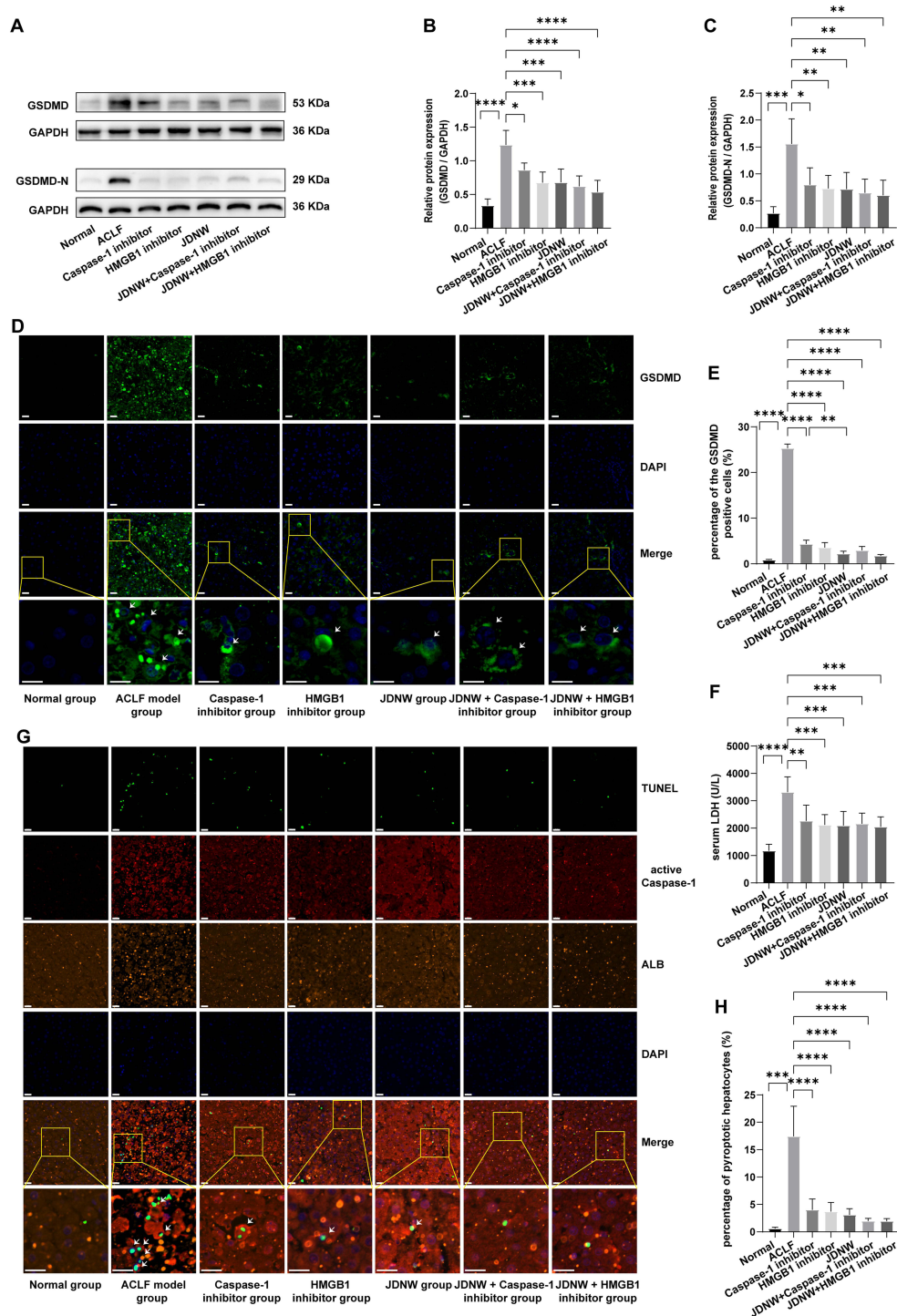


**Figure 5** JDNWF inhibited hepatocyte pyroptosis in ACLF rats.

**Notes:** (A–C) The Western blot was used to detect the expressions of GSDMD and GSDMD-N. GAPDH was used as the loading control.  $n=5$  per group. (D and E) The percentage of GSDMD-positive cells was detected by immunofluorescence (magnification,  $\times 400$ ; scale bar =  $20\mu\text{m}$ ). A region is selected randomly and further enlarged below (magnification,  $\times 1200$ ; scale bar =  $20\mu\text{m}$ ). The arrows indicate GSDMD-positive cells.  $n=5$  per group. (F) The serum LDH levels.  $n=7$  per group. (G and H) Triple-immunostaining of active Caspase-1, TUNEL and ALB were performed to further investigate hepatocyte pyroptosis in ACLF rats (magnification,  $\times 400$ ; scale bar =  $20\mu\text{m}$ ). A region is boxed randomly and further enlarged below (magnification,  $\times 1200$ ; scale bar =  $20\mu\text{m}$ ). The arrows represent pyroptotic hepatocytes.  $n=5$  per group. Asterisks indicate statistical significance:  $P^* < 0.05$ ,  $P^{**} < 0.01$ ,  $P^{***} < 0.001$ , and  $P^{****} < 0.0001$ .

**Abbreviations:** JDNWF, Jieduan-Niwan formula; ACLF, acute-on-chronic liver failure; GSDMD, Gasdermin D; LDH, lactate dehydrogenase; TUNEL, terminal deoxynucleotidyl transferase dUTP nick end labeling; ALB, albumin.

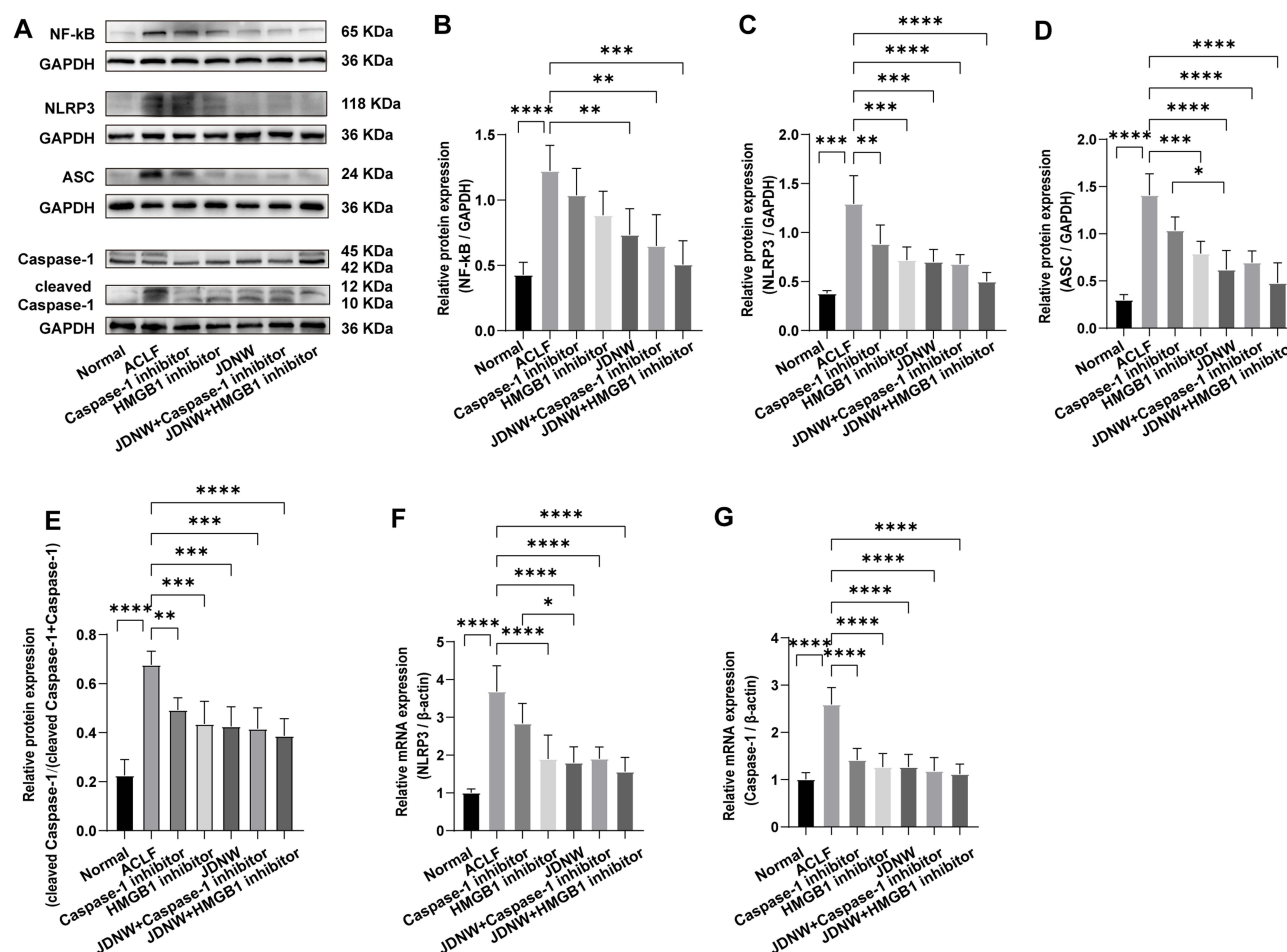


**Figure 6** JDNWF reduced hepatocyte pyroptosis in ACLF rats by inhibiting the HMGB1-induced pyroptosis pathways.

**Notes:** (A–E) The Western blot was used to detect the expressions of NF-κB, NLRP3, ASC, Caspase-1 and cleaved Caspase-1. GAPDH was used as the loading control. n=5 per group. (F and G) Relative transcript levels of *NLRP3* and *Caspase-1* were detected by the RT-qPCR. β-actin was used as internal reference. n=6 per group. Asterisks indicate statistical significance:  $P < 0.05$ ,  $P < 0.01$ ,  $P < 0.001$ , and  $P < 0.0001$ .

**Abbreviations:** JDNWF, Jieduan-Niwan formula; ACLF, acute-on-chronic liver failure; HMGB1, High mobility group box-1; NF-κB, nuclear factor kappa-light-chain-enhancer of activated B cells; ASC, the adaptor protein apoptosis-associated speck-like protein containing a caspase recruitment domain; RT-qPCR, quantitative real-time RT-PCR.

microbial invasion or tissue damage occurs.<sup>1,21</sup> Released into the local tissue environment and circulation, HMGB1 acquires a new identity as a DAMP molecule, which initiates pyroptosis via the upregulation of NF-κB-dependent pro-inflammatory cytokine secretion by binding to the HMGB1 receptor RAGE or TLR4, triggering and maintaining an inflammatory cascade.<sup>14</sup> Studies have shown that the serum HMGB1 level is significantly increased in patients with HBV-ACLF,<sup>15,22</sup> and there is HMGB1 translocation.<sup>22</sup> Considering that HMGB1 plays a critical role in ACLF, to further verify the mechanisms of the JDNWF and identify its potential molecular therapeutic targets, we evaluated the levels of HMGB1, RAGE and TLR4. As expected, we found that HMGB1 was activated in ACLF. Interestingly, the JDNWF significantly inhibited HMGB1, RAGE and TLR4 levels in liver and serum, as well as HMGB1 translocation, thereby inhibiting HMGB1 activation. Compared with GLY or VX-765, there were no significant differences after the JDNWF in combination with GLY or VX-765. These results strongly suggest that the JDNWF plays a hepatoprotective role by inhibiting HMGB1, which is an effective target of the JDNWF in the treatment of ACLF.

Considering that the activation of HMGB1 is closely related to pyroptosis,<sup>14</sup> GSDMD is cleaved during pyroptosis to form GSDMD-N, resulting in cell swelling and rupture, with the release of LDH and other intracellular substances, accompanied by pro-IL-1β and pro-IL-18 cleavage activation and the release of IL-1β, IL-18.<sup>14,16</sup> Pyroptosis is considered to trigger a large-scale inflammation, causing severe collateral damage to neighboring cells. To further elucidate the hepatoprotective mechanisms of the JDNWF, we investigated its effect on hepatocyte pyroptosis, and the results showed that the JDNWF inhibited the expressions of GSDMD, GSDMD-N, pro-IL-1β, IL-1β, IL-18 and the release of LDH, while decreasing the percentage of pyroptotic hepatocytes. Compared with GLY or VX-765, there were no significant differences in the above indicators after the JDNWF in





Taken together, this study further elucidates the part-molecular mechanisms of JDNWF treatment in ACLF. Our data suggest that the JDNWF plays a role in hepatoprotection by inhibiting the HMGB1-induced hepatocyte pyroptosis and reducing inflammatory responses.

## Conclusion

In summary, our data indicate that the JDNWF inhibits the HMGB1-induced hepatocyte pyroptosis to reduce inflammation, improve liver function, coagulation function and liver pathological damage in ACLF rats, and act as a liver protectant. This finding provides new and strong evidence for the efficacy of the JDNW in ACLF treatment.

## Abbreviations

ACLF, acute-on-chronic liver failure; ALB, albumin; ALT, alanine aminotransferase; ASC, the adaptor protein apoptosis-associated speck-like protein containing a caspase recruitment domain; AST, aspartate aminotransferase; CCl<sub>4</sub>, carbon tetrachloride; DAMPs, Damage-associated molecular patterns; DAPI, 4',6-diamidino-2-phenylindole; D-GalN, D-galactosamine; ELISA, enzyme-linked immunosorbent assay; ER, endoplasmic reticulum; GLY, glycyrrhizin; GSDMD, Gasdermin D; HE staining, hematoxylin and eosin staining; HMGB1, High mobility group box-1; IL-1 $\beta$ , interleukin-1  $\beta$ ; IL-6, interleukin-6; IL-18, interleukin-18; INR, international normalized ratio; i.g., intragastric administration; i.p., intraperitoneal injection; IVC, individually ventilated cage; JDNWF, Jieduan-Niwan formula; LDH, lactate dehydrogenase; LPS, Lipopolysaccharide; MT staining, masson's trichrome staining; MyD88, myeloid differentiation factor 88; NF- $\kappa$ B, nuclear factor kappa-light-chain-enhancer of activated B cells; PAMPs, Pathogen-associated molecular patterns; PT, prothrombin time; PVDF, polyvinylidene difluoride; RAGE, receptor for advanced glycation end-products; RT-qPCR, quantitative real-time RT-PCR; SDS-PAGE gel, SDS-polyacrylamide gel; SPF, specific-pathogen-free; TBIL, total bilirubin; TCM, traditional Chinese medicine; TEM, transmission electron microscopy; TLR4, Toll-like receptor 4; TNF- $\alpha$ , tumor necrosis factor- $\alpha$ ; TUNEL, terminal deoxynucleotidyl transferase dUTP nick end labeling.

## Ethical Approval

This study was approved by the Animal Ethics Committee of the Capital Medical University (approval ID: AEEI-2019-067), and all animal experiments were performed in accordance with the Guide for the Care and Use of Laboratory Animals of the Beijing Municipal Government.

## Acknowledgments

This study was supported by the National Natural Science Foundation of China [grant number 82074237 and 82270567] and the Beijing Municipal Natural Science Foundation [grant number 7244495].

## Disclosure

The authors report no conflicts of interest in this work.

## References

1. Kulkarni AV, Sarin SK. Acute-on-chronic liver failure - steps towards harmonization of the definition! *J Hepatol.* 2024;1–7. doi:10.1016/j.jhep.2024.03.036
2. Artru F, Trovato F, Morrison M, Bernal W, McPhail M. Liver transplantation for acute-on-chronic liver failure. *Lancet Gastroenterol Hepatol.* 2024;9(6):564–576. doi:10.1016/s2468-1253(23)00363-1
3. Hou W, Hao Y, Yang W, et al. The Jieduan-Niwan (JDNW) formula ameliorates hepatocyte apoptosis: a study of the inhibition of E2F1-mediated apoptosis signaling pathways in Acute-on-Chronic Liver Failure (ACLF) using rats. *Drug Des Devel Ther.* 2021;15:3845–3862. doi:10.2147/dddt.S308713
4. Wang X, Wang X. Guide lines for clinical diagnosis and treatment of acute-on-chronic liver failure in traditional Chinese medicine. *J Clin Hepatol.* 2019;35(03):494–503. doi:10.3969/j.issn.1001-5256.2019.03.009
5. Hu J, Qian Y, Yao N, et al. Treatment of chronic severe hepatitis B by Jieduan Niwan method. *Chin J Integr Tradit West Med Liver Dis.* 2010;20(04):200–203. doi:10.3969/j.issn.1005-0264.2010.04.003
6. Yang W, Hao Y, Hou W, et al. Jieduan-Niwan formula reduces liver apoptosis in a rat model of acute-on-chronic liver failure by regulating the E2F1-mediated intrinsic apoptosis pathway. *Evid Based Complement Alternat Med.* 2019;2019:8108503. doi:10.1155/2019/8108503



7. Fang P, Dou B, Hou W, et al. Jieduan-Niwan formula ameliorates oxidative stress and apoptosis in acute-on-chronic liver failure by Suppressing HMGB1/TLR-4/NF- $\kappa$ B signaling pathway: a study in vivo and in vitro. *Evid Based Complement Alternat Med.* **2022**;2022:1833921. doi:10.1155/2022/1833921
8. Fang X, Jiang X, Hou W, Fang P, Zhang Q. Study on the mechanism of Jieduan Niwan formula on cyclin D-E2F1 signaling pathway and transcription factor activation of rats with acute-on-chronic liver failure. *Global Tradit Chin Med.* **2021**;14(04):549–555. doi:10.3969/j.issn.1674-1749.2021.04.001
9. Liang J, Wei X, Hou W, et al. Liver metabolomics reveals potential mechanism of Jieduan-Niwan formula against acute-on-chronic liver failure (ACLF) by improving mitochondrial damage and TCA cycle. *Chin Med.* **2023**;18(1):157. doi:10.1186/s13020-023-00858-x
10. Moreau R, Tonon M, Krag A, Liver EAftSot. EASL clinical practice guidelines on acute-on-chronic liver failure. *J Hepatol.* **2023**;79(2):461–491. doi:10.1016/j.jhep.2023.04.021
11. Nguyen DV, Jin Y, Nguyen TLL, Kim L, Heo KS. 3'-Sialyllactose protects against LPS-induced endothelial dysfunction by inhibiting superoxide-mediated ERK1/2/STAT1 activation and HMGB1/RAGE axis. *Life Sci.* **2024**;338:122410. doi:10.1016/j.lfs.2023.122410
12. Deng C, Zhao L, Yang Z, et al. Targeting HMGB1 for the treatment of sepsis and sepsis-induced organ injury. *Acta Pharmacol Sin.* **2022**;43(3):520–528. doi:10.1038/s41401-021-00676-7
13. Zhang H, Xu G, Wu X, et al. Fei-Yan-Qing-Hua decoction decreases hyperinflammation by inhibiting HMGB1/RAGE signaling and promotes bacterial phagocytosis in the treatment of sepsis. *J Ethnopharmacol.* **2024**;321:117553. doi:10.1016/j.jep.2023.117553
14. Hou W, Wei X, Liang J, et al. HMGB1-induced hepatocyte pyroptosis expanding inflammatory responses contributes to the pathogenesis of Acute-on-Chronic Liver Failure (ACLF). *J Inflamm Res.* **2021**;14:7295–7313. doi:10.2147/jir.S336626
15. Zhao Q, Chen DP, Chen HD, et al. NK-cell-elicited gasdermin-D-dependent hepatocyte pyroptosis induces neutrophil extracellular traps that facilitate HBV-related acute-on-chronic liver failure. *Hepatology.* **2024**;81:917–931. doi:10.1097/hep.0000000000000868
16. Toldo S, Abbate A. The role of the NLRP3 inflammasome and pyroptosis in cardiovascular diseases. *Nat Rev Cardiol.* **2024**;21(4):219–237. doi:10.1038/s41569-023-00946-3
17. Taru V, Szabo G, Mehal W, Reiberger T. Inflammasomes in chronic liver disease: hepatic injury, fibrosis progression and systemic inflammation. *J Hepatol.* **2024**;81(5):895–910. doi:10.1016/j.jhep.2024.06.016
18. Xue R, Yang J, Jia L, et al. Mitofusin2, as a protective target in the liver, controls the balance of apoptosis and autophagy in acute-on-chronic liver failure. *Front Pharmacol.* **2019**;10:601. doi:10.3389/fphar.2019.00601
19. Xu Y, Wang Y, Qi R, et al. Role of connexin 32 in the directional differentiation of induced pluripotent stem cells into hepatocytes. *Int J Med Sci.* **2024**;21(3):508–518. doi:10.7150/ijms.83973
20. Schindelin J, Arganda-Carreras I, Frise E, et al. Fiji: an open-source platform for biological-image analysis. *Nat Methods.* **2012**;9(7):676–682. doi:10.1038/nmeth.2019
21. Chen R, Zou J, Zhong X, Li J, Kang R, Tang D. HMGB1 in the interplay between autophagy and apoptosis in cancer. *Cancer Lett.* **2024**;581:216494. doi:10.1016/j.canlet.2023.216494
22. Liu Y, Yuan W, Fang M, et al. Determination of HMGB1 in hepatitis B virus-related acute-on-chronic liver failure patients with acute kidney injury: early prediction and prognostic implications. *Front Pharmacol.* **2023**;13:1031790. doi:10.3389/fphar.2022.1031790

## Drug Design, Development and Therapy

### Publish your work in this journal

Drug Design, Development and Therapy is an international, peer-reviewed open-access journal that spans the spectrum of drug design and development through to clinical applications. Clinical outcomes, patient safety, and programs for the development and effective, safe, and sustained use of medicines are a feature of the journal, which has also been accepted for indexing on PubMed Central. The manuscript management system is completely online and includes a very quick and fair peer-review system, which is all easy to use. Visit <http://www.dovepress.com/testimonials.php> to read real quotes from published authors.

Submit your manuscript here: <https://www.dovepress.com/drug-design-development-and-therapy-journal>

**Dovepress**  
Taylor & Francis Group